

$b \rightarrow s\mu^+\mu^-$ anomalies and related phenomenology in $U(1)_{B_3-x_\mu L_\mu-x_\tau L_\tau}$ flavor gauge models

P. Ko^{a,b} Takaaki Nomura^a Chaehyun Yu^c

^a*School of Physics, KIAS, Seoul 02455, Korea*

^b*Quantum Universe Center, KIAS, Seoul 02455, Korea*

^c*Department of Physics, Korea University, Anam-ro 145, Sungbuk-gu, Seoul 02841, Korea*

E-mail: pko@kias.re.kr, nomura@kias.re.kr, chyu@korea.ac.kr

ABSTRACT: We propose a generation dependent lepton/baryon gauge symmetry, $U(1)_{B_3-x_\mu L_\mu-x_\tau L_\tau} \equiv U(1)_X$ (with $x_\mu+x_\tau=1$ for anomaly cancellation), as a possible solution for the $b \rightarrow s\mu^+\mu^-$ anomalies. By introducing two Higgs doublet fields, we can reproduce the observed CKM matrix, and generate flavor changing Z' interactions in the quark sector. Thus one can explain observed anomalies in $b \rightarrow s\ell^+\ell^-$ decay with the lepton non-universal $U(1)_X$ charge assignments. We show the minimal setup explaining $b \rightarrow s\ell^+\ell^-$ anomalies, neutrino masses and mixings and dark matter candidate, taking into account experimental constraints of flavor physics such as charged lepton flavor violations and the $B_s-\bar{B}_s$ mixing. Finally we discuss collider physics focusing on Z' production at the Large Hadron Collider and relic density of our dark matter candidate.

Contents

1	Introduction	1
2	Models and formulas	2
2.1	Discussion for general (x_μ, x_τ) case	3
2.1.1	Z' interactions with SM fermions	4
2.1.2	Effective interaction for $b \rightarrow s\mu^+\mu^-$	5
2.2	Minimal model	5
3	Neutrino mass and flavor constraints	9
3.1	Neutrino mass matrices	9
3.2	Charged lepton mass matrices	9
3.3	Charged lepton flavor violation	10
3.4	Constraint from neutrino trident process and Z' contribution to muon $g-2$	13
3.5	Constraint from $B_s-\bar{B}_s$ mixing	13
3.6	Prediction on $B \rightarrow K^{(*)}\tau^+\tau^-$	14
4	Collider physics and dark matter	14
4.1	Z' production at the LHC	15
4.2	Dark matter	16
5	Summary and discussions	18

1 Introduction

Although the standard model (SM) of particle physics is very successful we still do not have clear understanding of the physics regarding the flavors; namely the origin of fermion masses and mixing patterns. Then it is interesting to construct a model describing flavor physics with some symmetry as a guiding principle. One of the attractive possibility is an introduction of flavor dependent $U(1)$ gauge symmetry which can constrain structure of Yukawa couplings generating masses for quarks, charged leptons and neutrinos. In this kind of approaches to the flavor problem, these models may generate flavor changing neutral current (FCNC) processes through Z' boson exchange, which will induce rich phenomenology.

Recently there have been some indication of anomalies in B physics measurements for $b \rightarrow s\ell^+\ell^-$ process. The angular observable P'_5 in decay of B meson, $B \rightarrow K^*\mu^+\mu^-$ [1], indicates 3.4σ deviations from the data with integrated luminosity of 3.0 fb^{-1} at the LHCb [2], confirming an earlier observation with 3.7σ deviations [3]. In addition, 2.1σ deviations were

reported for the same observable by Belle [4, 5]. Furthermore, an anomaly in the measurement of lepton flavor universality by the ratio $R_K = BR(B^+ \rightarrow K^+ \mu^+ \mu^-) / BR(B^+ \rightarrow K^+ e^+ e^-)$ [6, 7] at the LHCb shows 2.6σ deviations from the SM prediction [8]. Moreover the LHCb collaboration also reported an anomaly in the ratio $R_{K^*} = BR(B \rightarrow K^* \mu^+ \mu^-) / BR(B \rightarrow K^* e^+ e^-)$ where the observed values are deviated from the SM prediction by $\sim 2.4\sigma$ as $R_{K^*} = 0.660_{-0.070}^{+0.110} \pm 0.024(0.685_{-0.069}^{+0.113} \pm 0.047)$ for $(2m_\mu^2) < q^2 < 1.1 \text{ GeV}^2$ ($1.1 \text{ GeV}^2 < q^2 < 6 \text{ GeV}^2$) [9].

These anomalies in the $b \rightarrow s \ell^+ \ell^-$ channels (with $\ell = e, \mu$) can be explained by flavor dependent Z' interactions inducing effective operator of $(\bar{b} \gamma^\alpha s)(\bar{\mu} \gamma_\alpha \mu)$, if new physics contribution to the corresponding Wilson coefficient C_9^μ is roughly $\Delta C_9^\mu \sim -1$ by global fits [10–13]. Then many models have been proposed to explain the anomalies by Z' interactions [14–44].

In this paper, motivated by $b \rightarrow s \ell^+ \ell^-$ anomalies, we propose a model based on flavor dependent Abelian gauge symmetry $U(1)_{B_3 - x_\mu L_\mu - x_\tau L_\tau}$, which is anomaly-free for $x_\mu + x_\tau = 1$. In this model we introduce two Higgs doublet fields to generate the realistic CKM matrix, where small mixings associated with third generation quarks can be obtained naturally as shown in Ref. [14]. In the reference it is also shown that $Z'bs$ interaction is induced after electroweak symmetry breaking in a model with flavor dependent $U(1)_{L_\mu - L_\tau - a(B_1 + B_2 - 2B_3)}$ gauge symmetry where a can be arbitrary real number. Then, $b \rightarrow s \ell^+ \ell^-$ anomalies can be explained by the effective operator induced by exchange of a TeV scale Z' boson. Following the same mechanism to induce $Z'bs$ interaction we can explain the anomalies by our flavor dependent $U(1)$ gauge symmetry if x_μ has negative value to get $\Delta C_9^\mu \sim -1$. We then consider the minimal model explaining $b \rightarrow s \ell^+ \ell^-$ anomalies and generating non-zero neutrino masses in which two SM singlet scalar fields are introduced. Also we introduce Dirac fermionic dark matter (DM) candidate in order to account for the dark matter of the Universe. In addition to ΔC_9^μ , we formulate neutrino mass matrix, lepton flavor violations (LFVs) and $B_s - \bar{B}_s$ mixing, and experimental constraints from them are taken into account. Then we discuss collider physics regarding Z' production at the Large Hadron Collider (LHC) and relic density of our DM candidate.

This paper is organized as follows. In Sec. II, we introduce our model and discuss quark mass, ΔC_9^μ by Z' and scalar masses in the minimal case. In Sec. III we discuss neutrino mass matrix, charged lepton flavor violations and $B_s - \bar{B}_s$ mixing taking into account experimental constraints. The numerical analysis is carried out in Sec. IV to discuss collider physics for Z' production at the LHC and relic density of DM candidate showing allowed parameter region. Finally summary and discussion are given in Sec. V.

2 Models and formulas

In this section we introduce our model based on flavor dependent $U(1)_{B_3 - x_\mu L_\mu - x_\tau L_\tau}$ gauge symmetry that we denote simply $U(1)_X$ in the following¹. The SM fermions with 3 right-handed (RH) neutrinos are charged under the $U(1)_X$ as shown in Table. 1. The gauge

¹In our analysis we ignore kinetic mixing between $U(1)_Y$ and $U(1)_X$ assuming it is sufficiently small.

Fermions	Q_{iL}	u_{iR}	d_{iR}	Q_{3L}	t_R	b_R	L_{1L}	L_{2L}	L_{3L}	e_R	μ_R	τ_R	ν_{1R}	ν_{2R}	ν_{3R}
$SU(3)_C$	3	3	3	3	3	3	1	1	1	1	1	1	1	1	1
$SU(2)_L$	2	1	1	2	1	1	2	2	2	1	1	1	1	1	1
$U(1)_Y$	$\frac{1}{6}$	$\frac{2}{3}$	$-\frac{1}{3}$	$\frac{1}{6}$	$\frac{2}{3}$	$-\frac{1}{3}$	$-\frac{1}{2}$	$-\frac{1}{2}$	$-\frac{1}{2}$	-1	-1	-1	0	0	0
$U(1)_X$	0	0	0	$\frac{1}{3}$	$\frac{1}{3}$	$\frac{1}{3}$	0	$-x_\mu$	$-x_\tau$	0	$-x_\mu$	$-x_\tau$	0	$-x_\mu$	$-x_\tau$

Table 1. Charge assignment for the SM fermions and right-handed neutrinos where the indices $i = 1, 2$ indicate the first and second generations.

anomalies are cancelled when the $U(1)_X$ charges of fermions satisfy the condition

$$x_\mu + x_\tau = 1, \quad (2.1)$$

which we will always assume in the following. In Sec. 2.1, we first discuss the case with general $x_{\mu,\tau}$ and investigate an explanation of $b \rightarrow s\ell^+\ell^-$ anomalies via flavor-changing Z' interactions. Then the minimal model with $x_\mu = -1/3$ is constructed in Sec. 2.2, taking into account the generation of active neutrino masses and mixings via Type-I seesaw mechanism.

2.1 Discussion for general (x_μ, x_τ) case

Firstly we consider quark sector which does not depend on our choice of x_μ and $x_\tau = 1 - x_\mu$. In this model we have to introduce at least two Higgs doublets in order to induce the realistic CKM mixing matrix:

$$\Phi_1 : (\mathbf{1}, \mathbf{2})(1/2, -1/3), \quad \Phi_2 : (\mathbf{1}, \mathbf{2})(1/2, 0), \quad (SU(3)_C, SU(2)_L)(U(1)_Y, U(1)_X) \quad (2.2)$$

Then the Yukawa couplings for quarks are given by

$$-\mathcal{L}_Q = y_{ij}^u \bar{Q}_{iL} \tilde{\Phi}_2 u_{jR} + y_{ij}^d \bar{Q}_{iL} \Phi_2 d_{jR} + y_{33}^u \bar{Q}_{3L} \tilde{\Phi}_2 t_R + y_{33}^d \bar{Q}_{3L} \Phi_2 b_R \\ + \tilde{y}_{3i}^u \bar{Q}_{3L} \tilde{\Phi}_1 u_{iR} + \tilde{y}_{i3}^d \bar{Q}_{iL} \Phi_1 b_R + \text{h.c.}, \quad (2.3)$$

where $i = 1, 2$ and $\tilde{\Phi}_i = i\sigma_2 \Phi_i^*$. Φ_2 is the Higgs doublet with vanishing $U(1)_X$ charge, and is the SM-like Higgs doublet. After two Higgs doublet fields get the non-zero vacuum expectation values (VEVs) $\langle \Phi_{1,2} \rangle = (0 \ v_{1,2}/\sqrt{2})^T$, we obtain the following forms of quark mass matrices:

$$M^u = \frac{1}{\sqrt{2}} \begin{pmatrix} v_2 y_{11}^u & v_2 y_{12}^u & 0 \\ v_2 y_{21}^u & v_2 y_{22}^u & 0 \\ 0 & 0 & v_2 y_{33}^u \end{pmatrix} + \begin{pmatrix} 0 & 0 & 0 \\ 0 & 0 & 0 \\ (\xi_u)_{31} & (\xi_u)_{32} & 0 \end{pmatrix}, \\ M^d = \frac{1}{\sqrt{2}} \begin{pmatrix} v_2 y_{11}^d & v_2 y_{12}^d & 0 \\ v_2 y_{21}^d & v_2 y_{22}^d & 0 \\ 0 & 0 & v_2 y_{33}^d \end{pmatrix} + \begin{pmatrix} 0 & 0 & (\xi_d)_{13} \\ 0 & 0 & (\xi_d)_{23} \\ 0 & 0 & 0 \end{pmatrix}. \quad (2.4)$$

Note that the matrices $(\xi_{u,d})_{ij} \equiv \tilde{y}_{ij}^{u,d} v_1/\sqrt{2}$ have the same structure as those discussed in Ref. [14]. We shall assume the second terms with $\xi_{u,d}$ are small perturbation effects

generating realistic 3×3 CKM mixing matrix where the (33) elements are $v_2 y_{33}^{u(d)} \sim \sqrt{2} m_{t(b)}$ following the discussion in Ref. [14].

As in the SM, the quark mass matrices are diagonalized by unitary matrices $U_{L,R}$ and $D_{L,R}$ which change quark fields from interaction basis to mass basis: $u_{L,R} \rightarrow U_{L,R}^\dagger u_{L,R}$ ($d_{L,R} \rightarrow D_{L,R}^\dagger d_{L,R}$). Then the CKM matrix is given by $V_{CKM} = U_L^\dagger D_L$. Thus we obtain relation between mass matrices $M^{u,d}$ and diagonalized ones as follows:

$$M^d = D_L m_{\text{diag}}^d D_R^\dagger, \quad M^u = U_L m_{\text{diag}}^u U_R^\dagger, \quad (2.5)$$

where diagonal mass matrices are given by $m_{\text{diag}}^d = \text{diag}(m_d, m_s, m_b)$ and $m_{\text{diag}}^u = \text{diag}(m_u, m_c, m_t)$. Then $U_{L[R]}$ and $D_{L[R]}$ are associated with diagonalization of $M^u (M^u)^\dagger [(M^u)^\dagger M^u]$ and $M^d (M^d)^\dagger [(M^d)^\dagger M^d]$ by

$$\begin{aligned} M^u (M^u)^\dagger [(M^u)^\dagger M^u] &= U_L^\dagger (m_{\text{diag}}^u)^2 U_L \left[U_R^\dagger (m_{\text{diag}}^u)^2 U_R \right], \\ M^d (M^d)^\dagger [(M^d)^\dagger M^d] &= D_L^\dagger (m_{\text{diag}}^d)^2 D_L \left[D_R^\dagger (m_{\text{diag}}^d)^2 D_R \right]. \end{aligned} \quad (2.6)$$

The structures of mass matrices in Eq. (2.4) indicate that the off-diagonal elements associated with 3rd generations are more suppressed for $M^u (M^u)^\dagger$ and $(M^d)^\dagger M^d$ than those in $(M^u)^\dagger M^u$ and $M^d (M^d)^\dagger$. More specifically, we find that

$$\begin{aligned} \left(M^u (M^u)^\dagger \right)_{31,32,13,23} \left[\left((M^d)^\dagger M^d \right)_{31,32,13,23} \right] &\propto \frac{v_2}{\sqrt{2}} y_{ij} \xi_{3k[k3]}, \\ \left((M^u)^\dagger M^u \right)_{31,32,13,23} \left[\left(M^d (M^d)^\dagger \right)_{31,32,13,23} \right] &\propto \frac{v_2}{\sqrt{2}} y_{33} \xi_{3k[k3]}, \end{aligned} \quad (2.7)$$

where $\{i, j, k\} = 1, 2$. Then we can approximate U_L and D_R to be close to unity matrix since they are associated with diagonalization of $M^u (M^u)^\dagger$ and $(M^d)^\dagger M^d$, respectively, where mixing angles in $D_R (U_L)$ generated by ξ parameters are suppressed by $m_{d,s(u,c)}/m_{b(t)}$ to those in $D_L (U_R)$. Therefore CKM matrix can be approximated as $V_{CKM} \simeq D_L$, and $D_R \simeq \mathbf{1}$, as obtained in Ref. [14]. Taking $D_L = V_{CKM}$, we can obtain sizes of $(\xi_d)_{13}$ and $(\xi_d)_{23}$ from Eq. (2.6) applying mass eigenvalues of down-type quarks. We thus obtain

$$|(\xi_d)_{13}| \sim 0.034 \text{ GeV}, \quad |(\xi_d)_{23}| \sim 0.18 \text{ GeV} \quad (2.8)$$

with $y_{33} v_2 / \sqrt{2} \simeq m_b \simeq 4.2 \text{ GeV}$. Therefore we can reconstruct mass eigenvalues of down-type quarks with $D_L \simeq V_{CKM}$ taking these values for ξ_d (values of y_{ij} are chosen to fit m_d and m_s). In addition, the values of ξ_u tend to be smaller than ξ_d due to mass relation $m_b \ll m_t$.

2.1.1 Z' interactions with SM fermions

The Z' couplings to the SM fermions are written as

$$\begin{aligned} \mathcal{L} \supset &-g_X (x_\mu \bar{\mu} \gamma^\mu \mu + x_\tau \bar{\tau} \gamma^\mu \tau + x_\mu \bar{\nu}_\mu \gamma^\mu P_L \nu_\mu + x_\tau \bar{\nu}_\tau \gamma^\mu P_L \nu_\tau + x_\mu \bar{\nu}_2 \gamma^\mu P_R \nu_2 + x_\tau \bar{\nu}_3 \gamma^\mu P_R \nu_3) Z'_\mu \\ &+ \frac{g_X}{3} \bar{t} \gamma^\mu t Z'_\mu + \frac{g_X}{3} \left(\bar{d}_\alpha \gamma^\mu P_L d_\beta \Gamma_{\alpha\beta}^{dL} + \bar{d}_\alpha \gamma^\mu P_R d_\beta \Gamma_{\alpha\beta}^{dR} \right) Z'_\mu, \end{aligned} \quad (2.9)$$

where g_X is the gauge coupling constant associated with the $U(1)_X$ and the lepton sector is given in the flavor basis here. The coupling matrices Γ^{dR} and Γ^{dL} for down-type quarks are given approximately by

$$\Gamma^{dL} \simeq \begin{pmatrix} |V_{td}|^2 & V_{ts}V_{td}^* & V_{tb}V_{td}^* \\ V_{td}V_{ts}^* & |V_{ts}|^2 & V_{tb}V_{ts}^* \\ V_{td}V_{tb}^* & V_{ts}V_{tb}^* & |V_{tb}|^2 \end{pmatrix}, \quad \Gamma^{dR} \simeq \begin{pmatrix} 0 & 0 & 0 \\ 0 & 0 & 0 \\ 0 & 0 & 1 \end{pmatrix}, \quad (2.10)$$

where $V_{qq'}$'s are the CKM matrix elements. We have applied the relation $V_{CKM} \simeq D_L$, as we discussed above. In our model the Z' mass, $m_{Z'}$, is dominantly given by the VEV of SM singlet scalar field as discussed below.

At this point, x_μ is an arbitrary parameter requiring only anomaly cancellation condition Eq. (2.1). This value will be fixed to obtain negative ΔC_9^μ and to realize minimal scalar sector. The mass of Z' can be a free parameter since it is given by new gauge coupling g_X and scalar singlet VEV where we have freedom to chose the VEV even if the gauge coupling is fixed.

2.1.2 Effective interaction for $b \rightarrow s\mu^+\mu^-$

Gauge interactions in Eq. (2.9) induce the effective Hamiltonian for $b \rightarrow s\mu^+\mu^-$ process such that

$$\begin{aligned} \Delta H_{\text{eff}} &= -\frac{x_\mu g_X^2 V_{tb}V_{ts}^*}{3m_{Z'}^2} (\bar{s}\gamma^\mu P_L b) (\bar{\mu}\gamma_\mu \mu) + h.c. \\ &= \frac{x_\mu g_X^2}{3m_{Z'}^2} \left(\frac{\sqrt{2}\pi}{G_F \alpha_{em}} \right) \left(\frac{-4G_F \alpha_{em}}{\sqrt{2}} \frac{V_{tb}V_{ts}^*}{4\pi} \right) (\bar{s}\gamma^\mu P_L b) (\bar{\mu}\gamma_\mu \mu) + h.c., \end{aligned} \quad (2.11)$$

where G_F is the Fermi constant and α_{em} is the electromagnetic fine structure constant. We thus obtain the Z' contribution to Wilson coefficient ΔC_9^μ as

$$\Delta C_9^\mu = \frac{x_\mu g_X^2}{3m_{Z'}^2} \left(\frac{\sqrt{2}\pi}{G_F \alpha_{em}} \right) \simeq 2.78 \times x_\mu \left(\frac{g_X}{0.62} \right)^2 \left(\frac{1.5 \text{ TeV}}{m_{Z'}} \right)^2. \quad (2.12)$$

In order to obtain $\Delta C_9^\mu \sim -1$, x_μ should be negative and g_X is required to be ~ 0.6 for $m_{Z'} = 1.5 \text{ TeV}$ and $x_\mu = -\frac{1}{3}$. Figure 1 shows the contour of ΔC_9^μ in the $(m_{Z'}, g_X)$ plane where we took $x_\mu = -\frac{1}{3}$ where the yellow(light-yellow) region corresponds to 1σ (2σ) region from global fit in Ref. [11].

2.2 Minimal model

Here we consider the minimal cases for choosing $U(1)_X$ charges of leptons as

$$x_\mu = -\frac{1}{3}, \quad x_\tau = \frac{4}{3}. \quad (2.13)$$

In this case we add two $SU(2)_L$ singlet scalar fields:

$$\varphi_1 : (\mathbf{1}, \mathbf{1})(0, 1/3), \quad \varphi_2 : (\mathbf{1}, \mathbf{1})(0, 1), \quad (2.14)$$

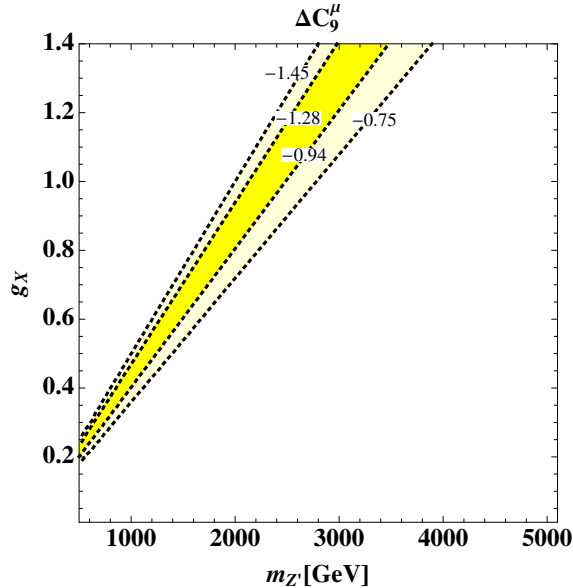


Figure 1. The contours showing Z' contribution to ΔC_9^μ on the $m_{Z'}-g_X$ plane with $x_\mu = -\frac{1}{3}$ where yellow(light-yellow) region corresponds to 1σ (2σ) region from global fit in Ref. [11].

Fields	Φ_1	Φ_2	φ_1	φ_2	χ
$SU(2)_L$	2	2	1	1	1
$U(1)_Y$	$\frac{1}{2}$	$\frac{1}{2}$	0	0	0
$U(1)_X$	$-\frac{1}{3}$	0	$\frac{1}{3}$	1	$\frac{5}{6}$

Table 2. Scalar fields and extra fermion χ in the minimal model and their representation under $SU(2) \times U(1)_Y \times U(1)_X$ where these fields are color singlet.

where φ_1 is also necessary to induce $\Phi_1^\dagger \Phi_2$ terms², while φ_2 is added for generating the 23(32) element of Majorana mass matrix of right-handed neutrino. Note that we obtain a massless Goldstone boson from two Higgs doublet sector without φ_1 due to an additional global symmetry. In addition we introduce additional Dirac fermion χ of mass m_χ with $U(1)_X$ charge $5/6$, which can be our DM candidate since its stability is guaranteed due to fractional charge assignment under $U(1)_X$. Note that the stability of Dirac fermion DM χ is guaranteed by remnant Z_2 symmetry after $U(1)_X$ symmetry breaking: particles with $U(1)_X$ charge $2n/6$ (n is integer) are Z_2 even and those with $U(1)_X$ charge $(2n+1)/6$ are Z_2 odd, since $U(1)_X$ symmetry is broken by VEVs of scalar fields φ_1 , φ_2 and Φ_1 whose charges correspond to $2n/6$ [47]. We summarize the charge assignment of scalar fields and new fermion in Table 2. In the later analysis, we will adopt this minimal setting.

²Note that we need one more scalar singlet to generate neutrino mass when $x_\mu \neq -1/3$.

In our set up, the full scalar potential for scalar fields in our model is given by

$$\begin{aligned}
V = & -\mu(\Phi_1^\dagger \Phi_2 \varphi_1^* + \text{h.c.}) + \mu_{11}^2 |\Phi_1|^2 + \mu_{22}^2 |\Phi_2|^2 + \mu_{\varphi_1}^2 |\varphi_1|^2 + \mu_{\varphi_2}^2 |\varphi_2|^2 \\
& + \frac{\lambda_1}{2} |\Phi_1|^4 + \frac{\lambda_2}{2} |\Phi_2|^4 + \lambda_3 |\Phi_1|^2 |\Phi_2|^2 + \lambda_4 |\Phi_1^\dagger \Phi_2|^2 + \lambda_{\varphi_1} |\varphi_1|^4 + \lambda_{\varphi_2} |\varphi_2|^4 \\
& + \lambda_{\Phi_1 \varphi_1} |\Phi_1|^2 |\varphi_1|^2 + \lambda_{\Phi_2 \varphi_1} |\Phi_2|^2 |\varphi_1|^2 + \lambda_{\Phi_1 \varphi_2} |\Phi_1|^2 |\varphi_2|^2 + \lambda_{\Phi_2 \varphi_2} |\Phi_2|^2 |\varphi_2|^2 + \lambda_{\varphi_1 \varphi_2} |\varphi_1|^2 |\varphi_2|^2 \\
& - \lambda_X (\varphi_1^3 \varphi_2^* + \text{h.c.}), \tag{2.15}
\end{aligned}$$

where we assumed all the coupling constants are real for simplicity. The VEVs of singlet scalar fields are written by $\sqrt{2}\langle\varphi_1\rangle = v_{\varphi_1}$ and $\sqrt{2}\langle\varphi_2\rangle = v_{\varphi_2}$. In our scenario, we assume $v_{\varphi_1}^2 \gg v_{\varphi_2}^2 \gg v_{1,2}^2$ and $U(1)_X$ symmetry is spontaneously broken at a scale higher than the electroweak scale. We then approximately obtain VEVs of $\varphi_{1,2}$ from the condition $\partial V/\partial v_{\varphi_{1,2}} = 0$:

$$v_{\varphi_1} \simeq \sqrt{\frac{-\mu_{\varphi_1}^2}{\lambda_{\varphi_1}}}, \quad v_{\varphi_2} \simeq \frac{\lambda_X v_{\varphi_1}^3}{4\mu_{\varphi_2}^2 + 2\lambda_{\varphi_1 \varphi_2} v_{\varphi_1}^2}, \tag{2.16}$$

where the above assumption for VEV hierarchy can be consistent requiring $\lambda_X v_{\varphi_1}^2 \ll \mu_{\varphi_2}^2$. Then the mass of the Z' boson is approximately given by

$$m_{Z'} \simeq \frac{1}{3} g_X v_{\varphi_1}. \tag{2.17}$$

Then a typical value of the φ_1 VEV is $v_{\varphi_1} \simeq 7.5 \times (m_{Z'}/1.5 \text{ TeV})(0.6/g_X) \text{ TeV}$ in our scenario. Note that the Z - Z' mass mixing is highly suppressed by $v_1^2/v_{\varphi_1}^2$ factor which is $\sim 10^{-5}$ for $\tan\beta = v_2/v_1 = 10$ and $v_{\varphi_1} = 7.5 \text{ TeV}$. Thus we will ignore this effect in our analysis³.

After $U(1)_X$ symmetry breaking, we obtain two-Higgs doublet potential effectively⁴:

$$\begin{aligned}
V_{THDM} = & m_1^2 |\Phi_1|^2 + m_2^2 |\Phi_2|^2 - (m_3^2 \Phi_1^\dagger \Phi_2 + \text{h.c.}) \\
& + \frac{\lambda_1}{2} |\Phi_1|^4 + \frac{\lambda_2}{2} |\Phi_2|^4 + \lambda_3 |\Phi_1|^2 |\Phi_2|^2 + \lambda_4 |\Phi_1^\dagger \Phi_2|^2, \tag{2.18}
\end{aligned}$$

$$m_{1(2)}^2 = \mu_{11(22)}^2 + \frac{1}{2} \lambda_{\Phi_{1(2)} \varphi_1} v_{\varphi_1}^2 + \frac{1}{2} \lambda_{\Phi_{1(2)} \varphi_2} v_{\varphi_2}^2, \quad m_3^2 = \frac{1}{\sqrt{2}} \mu v_{\varphi_1}. \tag{2.19}$$

Here we write Φ_i ($i = 1, 2$) as

$$\Phi_i = \begin{pmatrix} w_i^+ \\ \frac{1}{\sqrt{2}}(v_i + h_i + iz_i) \end{pmatrix}. \tag{2.20}$$

³The Z - Z' mixing effect is constrained by precision measurements of $Z\bar{f}_{SM}f_{SM}$ coupling at the LEP experiments where the upper bound of the mixing $\theta_{ZZ'}$ is around $\sim 10^{-3} - 10^{-4}$ [45, 46]. Thus our mixing angle is sufficiently smaller than the bound.

⁴Here we do not consider scalar bosons from $\varphi_{1,2}$ since they are assumed to be much heavier than those from Higgs doublets and mixing among singlet and doublet scalars will be small.

As in the two-Higgs-doublet model (THDM), we obtain mass eigenstate $\{H, h, A, H^\pm\}$ in the two Higgs doublet sector:

$$\begin{pmatrix} z_1(w_1^+) \\ z_2(w_2^+) \end{pmatrix} = \begin{pmatrix} \cos \beta & -\sin \beta \\ \sin \beta & \cos \beta \end{pmatrix} \begin{pmatrix} G_Z(G^+) \\ A(H^+) \end{pmatrix}, \quad (2.21)$$

$$\begin{pmatrix} h_1 \\ h_2 \end{pmatrix} = \begin{pmatrix} \cos \alpha & -\sin \alpha \\ \sin \alpha & \cos \alpha \end{pmatrix} \begin{pmatrix} H \\ h \end{pmatrix}, \quad (2.22)$$

where $\tan \beta = v_2/v_1$, $G_Z(G^+)$ is a Nambu-Goldstone boson (NG) absorbed by the $Z(W^+)$ boson, and h is the SM-like Higgs boson. The masses of H^\pm and A are given as in THDM:

$$m_{H^\pm}^2 = \frac{m_3^2}{\sin \beta \cos \beta} - \frac{v^2}{2} \lambda_4, \quad m_A^2 = \frac{m_3^2}{\sin \beta \cos \beta}. \quad (2.23)$$

Mass eigenvalues of CP-even scalar bosons are also obtained by

$$m_{H,h}^2 = \frac{1}{2} \left(M_1^2 + M_2^2 \pm \sqrt{(M_1^2 - M_2^2)^2 + 4M_{12}^4} \right), \quad (2.24)$$

$$M_1^2 = v^2(\lambda_1 \cos^4 \beta + \lambda_2 \sin^4 \beta) + \frac{v^2}{2} \bar{\lambda} \sin^2 2\beta, \quad (2.25)$$

$$M_2^2 = \frac{m_3^2}{\sin \beta \cos \beta} + v^2 \sin^2 \beta \cos^2 \beta (\lambda_1 + \lambda_2 - 2\bar{\lambda}), \quad (2.26)$$

$$M_{12}^2 = \frac{v^2}{2} \sin 2\beta (-\lambda_1 \cos^2 \beta + \lambda_2 \sin^2 \beta) + \frac{v^2}{2} \bar{\lambda} \sin 2\beta \cos 2\beta, \quad (2.27)$$

where $\bar{\lambda} = \lambda_3 + \lambda_4$ and lighter mass eigenvalue m_h is identified as the SM-like Higgs mass.

Note that Higgs bosons in doublet interact with Z' and three point couplings can be obtained such that

$$\begin{aligned} (D_\mu H_1)^\dagger (D^\mu H_1) &\supset i \frac{g_X}{3} Z'^\mu (w_1^+ \partial_\mu w_1^- - w_1^- \partial_\mu w_1^+) + \frac{2g_X}{3} Z'^\mu (h_1 \partial_\mu z_1 - z_1 \partial_\mu h_1) \\ &\supset i \frac{g_X \sin^2 \beta}{3} Z'^\mu (H^+ \partial_\mu H^- - H^- \partial_\mu H^+) + \frac{2g_X \sin \beta \sin \alpha}{3} Z'^\mu (h \partial_\mu A - A \partial_\mu h) \\ &\quad + \frac{2g_X \sin \beta \cos \alpha}{3} Z'^\mu (A \partial_\mu H - H \partial_\mu A). \end{aligned} \quad (2.28)$$

Thus Z' can decay into HA , hA and H^+H^- pair.

Here we briefly comment on deviation in the couplings of the SM-like Higgs h and constraint in the scalar sector in the model. The Yukawa interactions with h are given by Eq. (5.1) in the Appendix. In particular, we have flavor violating interaction associated with $\xi^{u,d}$ coupling. In our analysis, we assume the interactions are SM-like that can be realized taking large $\tan \beta$ and alignment limit of $\cos(\alpha - \beta) \simeq 0$. Note also that new scalar bosons do not contribute to explanation of $b \rightarrow s\mu^+\mu^-$ anomalies in our scenario except for relaxing the constraint from $B_s - \bar{B}_s$ mixing as we discuss below; we can fit the data with the mass value of ~ 500 to ~ 1000 GeV for exotic scalar bosons from two-Higgs doublet sector. In such a mass region, we can find a parameter to avoid collider constraints for exotic scalar production like that of charged scalar bosons [48]. We thus just assume new scalar bosons are sufficiently heavy and we can avoid constraints from scalar boson search at the LHC. Discussion of scalar sector can be referred to, for example, Refs. [14, 34].

3 Neutrino mass and flavor constraints

In this section we formulate neutrino mass matrices (both Dirac and Majorana mass matrices), and explore constraints from flavor physics such as $\mu \rightarrow e\gamma$, $\mu \rightarrow e$ conversion and $B_s-\bar{B}_s$ mixing.

3.1 Neutrino mass matrices

The Yukawa interactions for leptons are given by

$$-\mathcal{L} \supset y_{aa}^e \bar{L}_{aL} e_{aR} \Phi_2 + y_{aa}^\nu \bar{L}_{aL} \nu_{aR} \tilde{\Phi}_2 + \tilde{y}_{12}^e \bar{L}_{1L} \mu_R \Phi_1 + \tilde{y}_{21}^\nu \bar{L}_{2L} \nu_{1R} \tilde{\Phi}_1 + M \bar{\nu}_{1R}^c \nu_{1R} + Y_{12} \bar{\nu}_{1R}^c \nu_{2R} \varphi_1^* + Y_{23} \bar{\nu}_{2R}^c \nu_{3R} \varphi_2^* + h.c., \quad (3.1)$$

where $a = 1, 2, 3$ and $Y_{ab} = Y_{ba}$. After the symmetry breaking, Dirac and Majorana mass matrices for neutrinos have the structure of

$$M_D = \begin{pmatrix} (M_D)_{11} & 0 & 0 \\ (M_D)_{21} & (M_D)_{22} & 0 \\ 0 & 0 & (M_D)_{33} \end{pmatrix}, \quad M_{\nu_R} = \begin{pmatrix} (M_{\nu_R})_{11} & (M_{\nu_R})_{12} & 0 \\ (M_{\nu_R})_{21} & 0 & (M_{\nu_R})_{23} \\ 0 & (M_{\nu_R})_{32} & 0 \end{pmatrix}, \quad (3.2)$$

where the elements of the mass matrices are given by

$$(M_D)_{aa} = \frac{1}{\sqrt{2}} y_{aa}^\nu v_2, \quad (M_D)_{21} = \frac{1}{\sqrt{2}} \tilde{y}_{21} v_1, \\ (M_{\nu_R})_{11} = M, \quad (M_{\nu_R})_{12(21)} = \frac{1}{\sqrt{2}} Y_{12} v_{\varphi_1}, \quad (M_{\nu_R})_{23(32)} = \frac{1}{\sqrt{2}} Y_{23} v_{\varphi_2}. \quad (3.3)$$

The active neutrino mass matrix is given by type-I seesaw mechanism:

$$m_\nu \simeq -M_D M_{\nu_R}^{-1} M_D^T \\ = \begin{pmatrix} \frac{(M_D)_{11}^2}{(M_{\nu_R})_{11}} & \frac{(M_D)_{11}(M_D)_{21}}{(M_{\nu_R})_{11}} & -\frac{(M_D)_{11}(M_D)_{33}(M_{\nu_R})_{12}}{(M_{\nu_R})_{11}(M_{\nu_R})_{32}} \\ \frac{(M_D)_{11}(M_D)_{21}}{(M_{\nu_R})_{11}} & \frac{(M_D)_{21}^2}{(M_{\nu_R})_{11}} & \frac{(M_D)_{33}(M_D)_{22}}{(M_{\nu_R})_{32}} \left(1 - \frac{(M_D)_{21}(M_{\nu_R})_{12}}{(M_{\nu_R})_{11}(M_D)_{22}} \right) \\ -\frac{(M_D)_{11}(M_D)_{33}(M_{\nu_R})_{12}}{(M_{\nu_R})_{11}(M_{\nu_R})_{32}} & \frac{(M_D)_{33}(M_D)_{22}}{(M_{\nu_R})_{32}} \left(1 - \frac{(M_D)_{21}(M_{\nu_R})_{12}}{(M_{\nu_R})_{11}(M_D)_{22}} \right) & \frac{(M_D)_{33}^2 (M_{\nu_R})_{12}^2}{(M_{\nu_R})_{11}(M_{\nu_R})_{23}^2} \end{pmatrix}. \quad (3.4)$$

Note that our neutrino mass matrix does not have zero structure and neutrino oscillation data can be easily fit. Here we do not carry out further analysis of the neutrino phenomenology in this paper.

3.2 Charged lepton mass matrices

The charged lepton mass matrix is given by

$$M^e = \frac{1}{\sqrt{2}} \begin{pmatrix} y_{11}^e v_2 & \tilde{y}_{12}^e v_1 & 0 \\ 0 & y_{22}^e v_2 & 0 \\ 0 & 0 & y_{33}^e v_2 \end{pmatrix} \equiv \begin{pmatrix} m_{11}^e & \delta m_{12}^e & 0 \\ 0 & m_{22}^e & 0 \\ 0 & 0 & m_{33}^e \end{pmatrix}. \quad (3.5)$$

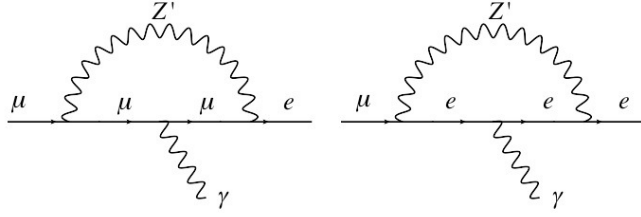


Figure 2. One loop diagrams inducing $\mu \rightarrow e\gamma$ process.

For $\delta m_{12}^e \ll m_{22}^e$, the mass matrix can be diagonalized in good approximation as

$$\begin{pmatrix} m_e & 0 & 0 \\ 0 & m_\mu & 0 \\ 0 & 0 & m_\tau \end{pmatrix} \simeq V_L^e M^e (V_R^e)^\dagger, \quad (3.6)$$

$$V_R^e \simeq \mathbf{1}, \quad V_L^e \simeq \begin{pmatrix} 1 & -\epsilon & 0 \\ \epsilon & 1 & 0 \\ 0 & 0 & 1 \end{pmatrix}, \quad (3.7)$$

where $\epsilon = \delta m_{12}^e / m_{22}^e$ we also find $m_e \simeq m_{11}^e$, $m_\mu \simeq m_{22}^e$ and $m_{33}^e = m_\tau$.

3.3 Charged lepton flavor violation

Here we consider charged lepton flavor violation (cLFV) in the model associated with Z' . The Z' gauge interactions for mass eigenstates of charged leptons are given by

$$\mathcal{L} \supset -\frac{g_X}{3} \bar{\ell}_i \gamma^\mu \left[V_L^e \begin{pmatrix} 0 & 0 & 0 \\ 0 & -1 & 0 \\ 0 & 0 & 4 \end{pmatrix} V_L^{e\dagger} \right]_{ij} P_L \ell_j Z'_\mu - \frac{g_X}{3} \bar{\ell}_i \gamma^\mu \begin{pmatrix} 0 & 0 & 0 \\ 0 & -1 & 0 \\ 0 & 0 & 4 \end{pmatrix}_{ij} P_R \ell_j Z'_\mu, \quad (3.8)$$

where the flavor violating structure for left-handed charged lepton currents is given by

$$V_L^e \begin{pmatrix} 0 & 0 & 0 \\ 0 & -1 & 0 \\ 0 & 0 & 4 \end{pmatrix} V_L^{e\dagger} \simeq \begin{pmatrix} -\epsilon^2 & \epsilon & 0 \\ \epsilon & -1 & 0 \\ 0 & 0 & 4 \end{pmatrix}. \quad (3.9)$$

Thus we have LFV interaction for e and μ . Then we first consider $\mu \rightarrow e\gamma$ process induced by Z' loop in Fig. 2 where the left diagram gives dominant contribution due to suppression by ϵ . Estimating the loop diagram we obtain dominant contribution to the decay width for the $\mu \rightarrow e\gamma$ process such that

$$\Gamma_{\mu \rightarrow e\gamma} \simeq \frac{e^2 m_\mu^3}{16\pi} |a_R|^2, \quad (3.10)$$

$$a_R \simeq \frac{e\epsilon g_X^2 m_\mu}{144\pi^2} \int_0^1 dx dy dz \delta(1-x-y-z) \frac{2x(1+y)}{[(x^2-x)+xz+y+z]m_\mu^2 + xm_{Z'}^2}. \quad (3.11)$$

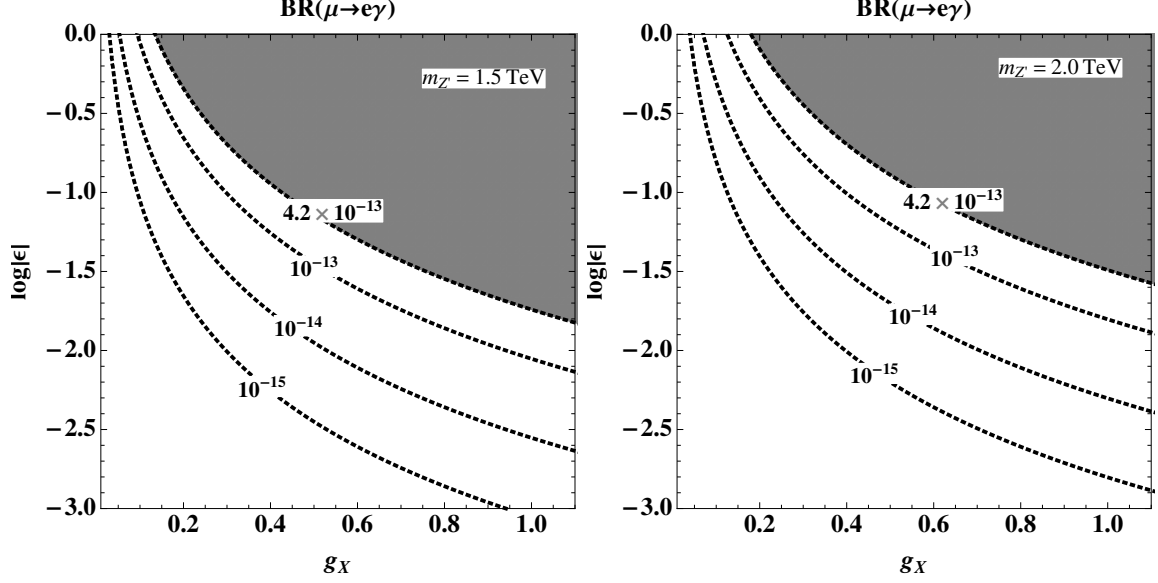


Figure 3. $BR(\mu \rightarrow e\gamma)$ as a function of $\{g_X, \log|\epsilon|\}$ fixing $m_{Z'} = 1.5(2.0)$ TeV for left(right) plot where the shaded regions are excluded.

Branching ratio for the LFV process is given by

$$BR(\mu \rightarrow e\gamma) = \frac{\Gamma_{\mu \rightarrow e\gamma}}{\Gamma_{\mu \rightarrow e\nu_e\nu_\mu}} \simeq \frac{12\alpha}{G_F^2 m_\mu^2} |a_R|^2, \quad (3.12)$$

where $G_F \simeq 1.17 \times 10^{-5} \text{ GeV}^{-2}$ is the Fermi constant and $\alpha \simeq 1/137$ is the fine structure constant. In Fig. 3, we show $BR(\mu \rightarrow e\gamma)$ on $\{g_X, \log|\epsilon|\}$ plane fixing $m_{Z'} = 1.5(2.0)$ TeV where the shaded regions are excluded by the current constraint $BR(\mu \rightarrow e\gamma) \lesssim 4.2 \times 10^{-13}$ by the MEG experiment [49]. Further parameter region will be explored in future with improved sensitivity [50].

Here we also discuss $\mu \rightarrow e$ conversion via Z' exchange. In our case, the relevant effective Lagrangian for the process is derived as follows [51–53]

$$\mathcal{L}_{eff} = -\frac{4G_F}{\sqrt{2}} \sum_{N=p,n} [C_{VL}^{NN} \bar{e}\gamma^\alpha P_L \mu \bar{N} \gamma_\alpha N + C_{AL}^{NN} \bar{e}\gamma^\alpha P_L \mu \bar{N} \gamma_\alpha \gamma_5 N], \quad (3.13)$$

where the corresponding coefficients are given by

$$C_{VL}^{pp(nn)} = -C_{AL}^{pp(nn)} = (2) \frac{\sqrt{2}\epsilon g_X^2 |V_{td}|^2}{216G_F m_{Z'}^2}. \quad (3.14)$$

Then we obtain the spin-independent contribution to the BR for $\mu \rightarrow e$ conversion on a nucleus such that

$$BR(\mu \rightarrow e) = \frac{32G_F^2 m_\mu^5}{\Gamma_{cap}} \left| C_{VL}^{pp} V^{(p)} + C_{VL}^{nn} V^{(n)} \right|^2, \quad (3.15)$$

Nucleus $\frac{A}{Z}N$	V^p	V^n	$\Gamma_{\text{capt}} [10^6 \text{sec}^{-1}]$
$^{27}_{13}\text{Al}$	0.0161	0.0173	0.7054
$^{197}_{79}\text{Au}$	0.0974	0.146	13.07

Table 3. A summary of parameters for the $\mu - e$ conversion formula for $^{27}_{13}\text{Al}$ and $^{197}_{79}\text{Au}$ nuclei [52, 54].

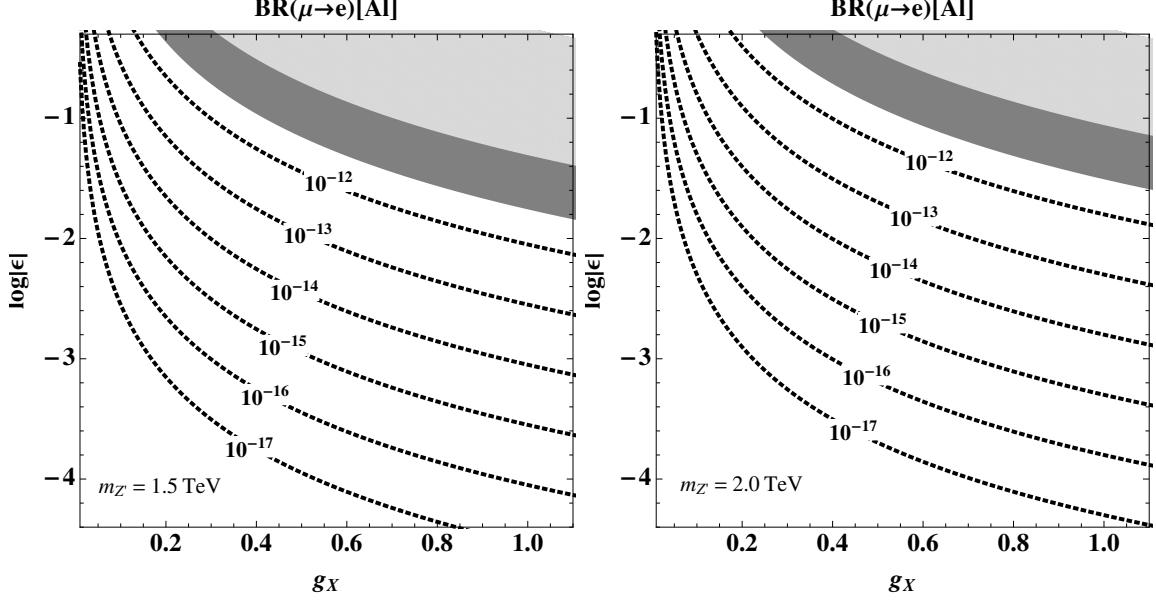


Figure 4. $BR(\mu \rightarrow e)$ on $^{27}_{13}\text{Al}$ as a function of $\{g_X, \log|\epsilon|\}$ fixing $m_{Z'} = 1.5(2.0)$ TeV for left(right) plot where gray(light-gray) shaded region is excluded by current $\mu \rightarrow e\gamma$ BR ($\mu \rightarrow e$ BR on $^{197}_{79}\text{Au}$ [55]) constraints.

where Γ_{cap} is the rate for the muon to transform to a neutrino by capture on the nucleus, and $V^{(p,n)}$ is the integral over the nucleus for lepton wavefunctions with corresponding nucleon density. The values of Γ_{cap} and $V^{(n,p)}$ depend on target nucleus and those for $^{197}_{79}\text{Au}$ and $^{27}_{13}\text{Al}$ are given in Table. 3 [52, 54]. In Fig. 4, we show $BR(\mu \rightarrow e)$ for $^{27}_{13}\text{Al}$ on $\{g_X, \log|\epsilon|\}$ plane fixing $m_{Z'} = 1.5(2.0)$ TeV in left(right)-panel where gray(light-gray) shaded region is excluded by current $\mu \rightarrow e\gamma$ BR ($\mu \rightarrow e$ BR on $^{197}_{79}\text{Au}$ [55]) constraints. We find that large parameter region can be explored by $\mu \rightarrow e$ conversion measurement since its sensitivity will reach $\sim 10^{-16}$ on $^{27}_{13}\text{Al}$ nucleus in future experiments [56, 57].

We next consider the LFV B decay $B_s \rightarrow \mu^\pm e^\mp$ which is related to C_9^μ above. It is because that the process is induced from $C_{10}^{\mu e}$ which is obtained as $C_{10}^{\mu e} = -\epsilon \Delta C_9^\mu$ in the model. The branching ratio can be given by

$$BR(B_s \rightarrow \mu e) = \left| \frac{C_{10}^{\mu e}}{C_{10}^{SM}} \right|^2 BR(B_s \rightarrow \mu^+ \mu^-)_{SM} \simeq |0.24 \times \epsilon \Delta C_9^\mu|^2 BR(B_s \rightarrow \mu^+ \mu^-)_{SM}, \quad (3.16)$$

where we used $C_{10}^{SM}(\mu_b) \simeq -4.2$ and $BR(B_s \rightarrow \mu^+ \mu^-)_{SM} = (3.65 \pm 0.23) \times 10^{-9}$ is the

SM prediction for the BR of $B_s \rightarrow \mu^+ \mu^-$. We find that $BR(B_s \rightarrow \mu e) < 10^{-11}$ in the parameter region satisfying the constraint from $BR(\mu \rightarrow e \gamma)$ which is well below the current constraint.

Here we also discuss the branching ratio for $B \rightarrow K^{(*)} \mu e$ through lepton flavor violating Z' coupling. It is suppressed compared to $BR(B \rightarrow K^{(*)} \mu \mu)$ by a factor of $|\epsilon \Delta C_9^\mu / C_9^\mu|^2 \sim 10^{-3}$ for $\Delta C_9^\mu = -1$ and $\epsilon = 0.1$. Thus the BR is small as order of $10^{-10} - 10^{-9}$ and it is well below current bound and challenging to search for the signal at the future experiments such as (upgraded) LHCb [58] and Belle II [59].

3.4 Constraint from neutrino trident process and Z' contribution to muon $g - 2$

$U(1)_X$ gauge coupling and Z' mass are constrained by the neutrino trident process $\nu N \rightarrow \nu N \mu^+ \mu^-$ where N is a nucleon [60]. The bound is approximately given by $m_{Z'}/g_X \gtrsim 550$ GeV for $m_{Z'} > 1$ GeV. We then consider parameter region of $\{m_{Z'}, g_X\}$ satisfying this bound.

The observed muon magnetic dipole moment is deviated from the SM prediction as $\Delta a_\mu = (26.1 \pm 8.0) \times 10^{-10}$ [61] (muon $g - 2$). The Z' boson can contribute to muon $g - 2$ at one loop level as

$$\Delta a_\mu^{Z'} \approx \frac{g_X^2 x_\mu^2}{4\pi^2} \int_0^1 da \frac{ra(1-a)^2}{r(1-a)^2 + a}, \quad (3.17)$$

where $r \equiv (m_\mu/M_{Z'})^2$. We find that the Z' contribution is small for the parameter region providing $\Delta C_9 \sim -1$; for example $\Delta a_\mu^{Z'} \sim 1.7 \times 10^{-12}$ with $m_{Z'} = 1500$ GeV and $g_X = 0.6$.

3.5 Constraint from $B_s - \bar{B}_s$ mixing

In our model, Z' and neutral scalar bosons induce flavor changing neutral current (FCNC) interactions. Here we consider constraints from $B_s - \bar{B}_s$ mixing where other $\Delta F = 2$ processes are more suppressed by CKM factors.

The effective Hamiltonian for the $B_s - \bar{B}_s$ mixing is given by

$$H_{eff} = C_1 (\bar{s} \gamma^\mu P_L b) (\bar{s} \gamma_\mu P_L b) + C_2' (\bar{s} P_R b) (\bar{s} P_R b). \quad (3.18)$$

The relevant Wilson coefficients are

$$C_1 = \frac{1}{2} \frac{g_X^2}{9m_{Z'}^2} (\Gamma_{sb}^{d_L})^2, \quad C_2' = \sum_{\eta=h,H,A} \frac{-1}{2m_\eta^2} (\Gamma_{sb}^\eta)^2, \quad (3.19)$$

where $\Gamma_{qq'}^\eta$ is couplings for $\eta \bar{q} q'$ interactions ($\eta = h, H, A$), the explicit expressions of which are given in the Appendix. Using these Wilson coefficients we obtain ratio between Δm_{B_s}

in our model and the SM prediction $\Delta m_{B_s}^{SM}$, under large $\tan\beta$ and small α , such that

$$\begin{aligned}
R_{B_s} &= \frac{\Delta m_{B_s}}{\Delta m_{B_s}^{SM}} \\
&\simeq \frac{g_X^2 (V_{tb} V_{ts}^*)^2}{9m_{Z'}^2} (8.2 \times 10^{-5} \text{ TeV}^{-2})^{-1} \\
&+ \left[0.12 \cos^2(\alpha - \beta) \tan^2 \beta + 0.19 \tan^2 \beta \left(\frac{(200 \text{ GeV})^2}{m_H^2} - \frac{(200 \text{ GeV})^2}{m_A^2} \right) \right], \quad (3.20)
\end{aligned}$$

where the first and second terms in the right-hand side corresponds to contributions from Z' and scalars, respectively [14, 62, 63]. The allowed range of R_{B_s} is estimated by [62, 63]

$$0.83 < R_{B_s} < 0.99. \quad (3.21)$$

We find that R_{B_s} will be deviated from the allowed range by Z' contribution when $\Delta C_9^\mu \simeq -1$ is required. Thus cancellation between Z' and scalar contribution is necessary to satisfy the experimental constraint⁵. Here we derive allowed parameter region on $\{m_H, m_A - m_H\}$ plane satisfying $B_s - \bar{B}_s$ constraints when we fit C_9^μ to explain $b \rightarrow s \ell^+ \ell^-$ anomalies choosing $\tan\beta = 10$ and $\cos(\alpha - \beta) \sim 0$ as reference values. In Fig. 5, we show the allowed parameter region where the yellow(light yellow) region corresponds to that in Fig. 1.

3.6 Prediction on $B \rightarrow K^{(*)} \tau^+ \tau^-$

Here we discuss $B \rightarrow K^{(*)} \tau^+ \tau^-$ process in our model. The branching ratios are given by Wilson coefficient C_9 associated with τ such that [68]

$$\begin{aligned}
10^7 \times BR(B \rightarrow K \tau^+ \tau^-)^{[15,22]} &= (1.20 + 0.15 \Delta C_9^\tau + 0.02 (\Delta C_9^\tau)^2) \\
&\pm (0.12 + 0.02 \Delta C_9^\tau), \quad (3.22)
\end{aligned}$$

$$\begin{aligned}
10^7 \times BR(B \rightarrow K^* \tau^+ \tau^-)^{[15,19]} &= (0.98 + 0.38 \Delta C_9^\tau + 0.05 (\Delta C_9^\tau)^2) \\
&\pm (0.09 + 0.03 \Delta C_9^\tau + 0.01 (\Delta C_9^\tau)^2), \quad (3.23)
\end{aligned}$$

where the superscript indicates the q^2 range for the dilepton invariant mass in unit of $[\text{GeV}^2]$. For the $b \rightarrow s \tau^+ \tau^-$ channel, we obtain $\Delta C_9^\tau = -4C_9^\mu$ from our charge assignments, and the BRs are slightly enhanced from the SM prediction by factor ~ 1.5 . However current upper bounds of the BRs are much larger than the prediction as $BR(B \rightarrow K \tau^+ \tau^-) < 2.25 \times 10^{-3}$ [69]. Therefore it is difficult to test the enhancement effect.

4 Collider physics and dark matter

In this section we explore collider physics focusing on Z' production at the LHC and estimate relic density of our DM candidate searching for parameter region providing observed value.

⁵ Similar phenomena were also observed in the flavor gauge model where $U(1)'$ gauge interaction couples only to the right-handed top quark in the interaction basis in the context of the top forward-backward asymmetry and the same sign top pair productions at hadron colliders [64–67]. In that model, cancellation between the amplitudes with t -channel exchanges of vector and (pseudo)scalar bosons occur in the same sign top pair production through $u_R u_R \rightarrow t_R t_R$, which saves the $U(1)$ flavor model from the stringent constraints from the same sign top pair production at the Tevatron and the LHC.

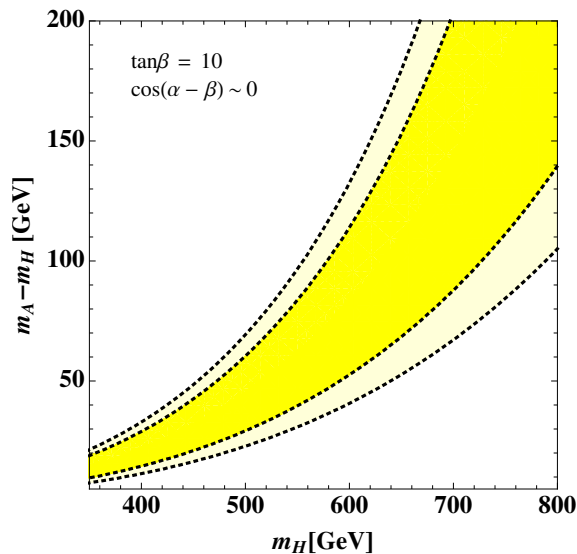


Figure 5. The allowed region on $\{m_H, m_A - m_H\}$ plane satisfying $B_s - \bar{B}_s$ constraints with fitting C_9 to explain $b \rightarrow s\ell^+\ell^-$ anomalies where the yellow(light yellow) region corresponds to that in Fig. 1. Here we take $\tan\beta = 10$ and $\cos(\alpha - \beta) \sim 0$ as reference values.

4.1 Z' production at the LHC

Here we discuss Z' production at the LHC 13 TeV where Z' can be produced via interaction in Eq. (2.9), followed by decay modes of $Z' \rightarrow \mu^+\mu^-$ and $Z' \rightarrow \tau^+\tau^-$ [Drell-Yan (DY) productions]. In this model Z' mainly decays into $\tau^+\tau^-$ model with $BR(Z' \rightarrow \tau^+\tau^-) \sim 0.5$ and BR of $\mu^+\mu^-$ mode is suppressed by factor of 1/16. The production cross section is estimated by CalcHEP [70] using the CTEQ6 parton distribution functions (PDFs) [71]. In Fig. 6, we show $\sigma(pp \rightarrow Z')BR(Z' \rightarrow \ell^+\ell^-/\tau^+\tau^-)$ ($\ell = e, \mu$) as a function of the Z' mass for several values of g_X . The cross sections are compared with constraints from LHC data; from Refs. [72] and [73] for $\ell^+\ell^-$ and $\tau^+\tau^-$ modes. We thus find that $\ell^+\ell^-$ mode (mostly $\mu^+\mu^-$) provides more strict bound although $BR(Z' \rightarrow \mu^+\mu^-) : BR(Z' \rightarrow \tau^+\tau^-) = 1 : 16$. Here we set masses of H , A and H^\pm as 400 GeV and apply $\tan\beta = 10$ and $\cos(\alpha - \beta) = 0$ where the effects of the Z' decays into scalar bosons are small. Also right-handed neutrinos and DM χ are taken to be heavier than $m_{Z'}/2$ so that Z' does not decay into on-shell right-handed neutrinos and DM.

Our Z' boson also decays into neutrinos with BR value of $BR(Z' \rightarrow \nu_\tau\bar{\nu}_\tau) = 16BR(Z' \rightarrow \nu_\mu\bar{\nu}_\mu) \simeq 0.25$. Thus we can also test our model by $pp \rightarrow Z'g \rightarrow \nu\bar{\nu}g$ process at the LHC experiments searching for signal with mono-jet plus missing transverse momentum. The cross section of $pp \rightarrow Z'g \rightarrow \nu\bar{\nu}g$ process is, for example, ~ 1 fb with $g_X = 0.6$ and $m_{Z'} = 1500$ GeV estimated by CalcHEP with $p_T > 25$ GeV cut. We thus need large integrated luminosity to analyze the signal [74] and it will be tested in future LHC experiments.

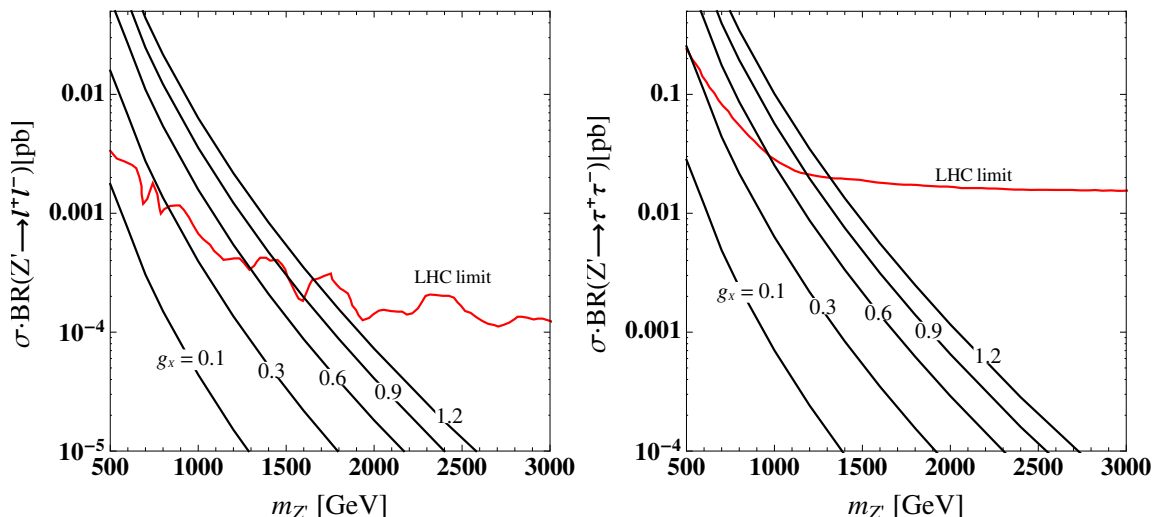


Figure 6. Left(right) plot: $\sigma(pp \rightarrow Z')BR(Z' \rightarrow \ell^+\ell^-(\tau^+\tau^-))$ with $\ell = e, \mu$ for several values of g_X compared with LHC limit; from Refs. [72] and [73] for $\ell^+\ell^-$ and $\tau^+\tau^-$ modes.

4.2 Dark matter

We consider a Dirac fermion χ as our DM candidate, and the relic density is determined by the DM annihilation process $\chi\bar{\chi} \rightarrow Z' \rightarrow f_{SM}\bar{f}_{SM}/HA/H^+H^-$ where f_{SM} is a SM fermion and/or $\chi\bar{\chi} \rightarrow Z'Z'$ depending on kinematic condition. Then we estimate relic density of our DM using `micrOMEGAs 4.3.5` [75] implementing relevant interactions. Fig. 7 shows the relic density Ωh^2 as a function of DM mass m_X where we apply several values of g_X and $m_{Z'} = 1.5$ TeV as reference values, and indicate observed Ωh^2 value by horizontal dashed line [76]. We see that the relic density drops at around $m_{Z'} \sim 2m_X$ due to resonant enhancement of the annihilation cross section.

In addition, we scan parameters in the range of

$$m_X \in [200, 3100] \text{ GeV}, \quad m_{Z'} \in [500, 7000] \text{ GeV}, \quad g_X \in [0.01, 1.5], \quad (4.1)$$

with assuming that $\tan\beta = 10$ and $\cos(\alpha - \beta) = 0$ as reference values. We note that the effects of scalar bosons are subdominant. The left panel of Fig. 8 shows the parameter region which accommodates the observed relic density of DM, $\Omega h^2 = 0.1206 \pm 0.0063$, taking 3σ range of observed value by the Planck collaboration [76]. Moreover the right panel of the figure indicates the region in which both observed relic density and $b \rightarrow s\ell^+\ell^-$ anomalies are explained within 2σ . Notice that the allowed region with $m_{Z'} < m_X$ is partly excluded by or close to LHC constraint shown in Fig. 6 and will be explored in future LHC experiments. In addition DM-nucleon scattering cross section by Z' exchange is suppressed by CKM factor and the allowed region is not constrained by the DM direct detection experiments.

Before closing this section we discuss possibility of indirect detection of our DM. In this model DM pair annihilates mainly through $\chi\bar{\chi} \rightarrow Z' \rightarrow \tau^+\tau^-$ and/or $\chi\bar{\chi} \rightarrow Z'Z' \rightarrow 2\tau^+\tau^-$

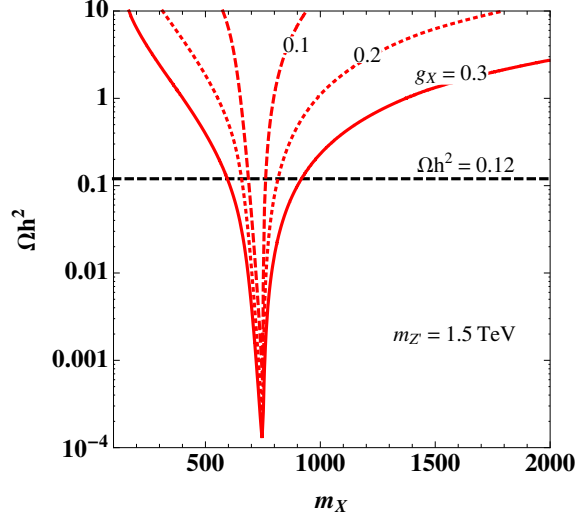


Figure 7. Relic density of DM as function of DM masses for different values of $U(1)_X$ gauge couplings, $g_X = 0.1, 0.2$ and 0.3 . We have fixed $m_{Z'} = 1.5$ TeV.

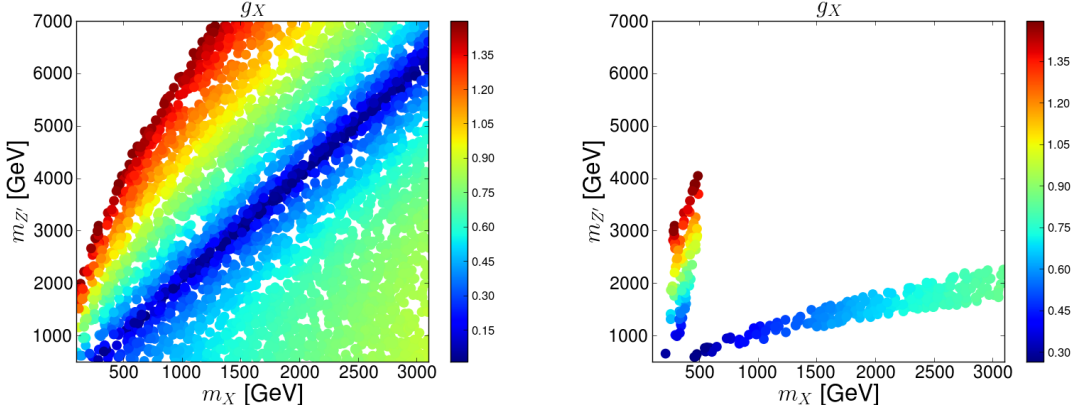


Figure 8. (Left): parameter region which accommodates the observed DM relic density. (Right): parameter region which explains both DM relic density and $b \rightarrow sl^+l^-$ anomalies.

and gamma-ray search gives the strongest constraint on the annihilation cross section by Fermi-LAT observation [77, 78]. In our parameter region of $m_{Z'} > 500$ GeV, DM annihilation cross section explaining the relic density is well below the constraint for the $\tau^+\tau^-$ dominant case [77, 78] unless there is large enhancement factor; constraint on cross section for four τ mode would be similar. Thus our model is safe from indirect detection cross section and will be tested with larger amount of data in future.

5 Summary and discussions

We have discussed a flavor model based on $U(1)_{B_3-x_\mu L_\mu-x_\tau L_\tau} (\equiv U(1)_X)$ gauge symmetry in which two Higgs doublet fields are introduced to obtain the observed CKM matrix. Flavor changing Z' interactions with the SM quarks are obtained after diagonalizing quark mass matrix, and $b \rightarrow s\ell^+\ell^-$ anomalies can be explained due to lepton flavor non-universal charge assignment when x_μ is taken to be negative value. Then we have considered minimal set up explaining $b \rightarrow s\ell^+\ell^-$ anomalies and generated neutrino mass matrix where two SM singlet scalar fields and Dirac fermionic DM candidate are introduced.

We have computed the Z' contribution to the Wilson coefficient C_9^μ relevant for $b \rightarrow s\mu^+\mu^-$, as well as neutrino mass matrices, charged lepton flavor violations and the $B_s-\bar{B}_s$ mixing, including the relevant experimental constraints. We have found that cancellation between Z' and scalar bosons contributions to $B_s-\bar{B}_s$ is required to satisfy experimental constraint, while explaining $b \rightarrow s\ell^+\ell^-$ anomalies. In addition, we have shown constraints from lepton flavor violation process $\mu \rightarrow e\gamma$ and future prospects for $\mu \rightarrow e$ conversion measurements.

Then collider physics regarding Z' production at the LHC and relic density of DM are explored. We have shown cross sections for the DY processes, $pp \rightarrow Z' \rightarrow \mu^+\mu^-(\tau^+\tau^-)$, where constraints on the $\{m_{Z'}, g_X\}$ parameter space dominantly come from the data of di-muon resonance search at the LHC. The relic density of DM further constrains $\{m_{Z'}, g_X\}$ parameter space since the relic density is determined by DM pair annihilation process via Z' interactions. The preferred parameter region can be further tested in future LHC experiments and observations for flavor physics such as LFVs.

Acknowledgments

The work of CY was supported by the National Research Foundation of Korea(NRF) grant funded by the Korea government(MSIT), NRF-2017R1A2B4011946 and NRF-2017R1E1A1A01074699.

Appendix: Yukawa interactions

Here we summarize Yukawa interactions in two Higgs doublet sector which are taken from ref. [14].

$$\begin{aligned}
\mathcal{L}_Y = & -\bar{u}_L \left(\frac{\cos\alpha}{v\sin\beta} m_u^D - \frac{\cos(\alpha-\beta)}{\sqrt{2}\sin\beta} \tilde{\xi}^u \right) u_R h - \bar{d}_L \left(\frac{\cos\alpha}{v\sin\beta} m_d^D - \frac{\cos(\alpha-\beta)}{\sqrt{2}\sin\beta} \tilde{\xi}^d \right) d_R h \\
& -\bar{u}_L \left(\frac{\sin\alpha}{v\sin\beta} m_u^D - \frac{\sin(\alpha-\beta)}{\sqrt{2}\sin\beta} \tilde{\xi}^u \right) u_R H - \bar{d}_L \left(\frac{\sin\alpha}{v\sin\beta} m_d^D - \frac{\sin(\alpha-\beta)}{\sqrt{2}\sin\beta} \tilde{\xi}^d \right) d_R H \\
& -i\bar{u}_L \left(\frac{m_u^D}{v\tan\beta} - \frac{1}{\sqrt{2}\sin\beta} \tilde{\xi}^u \right) u_R A + i\bar{d}_L \left(\frac{m_d^D}{v\tan\beta} - \frac{1}{\sqrt{2}\sin\beta} \tilde{\xi}^d \right) d_R A \\
& - \left[\bar{u}_R \left(\frac{\sqrt{2}}{v\tan\beta} m_u^D V - \frac{1}{\sin\beta} (\tilde{\xi}^u)^\dagger \right) d_L + \bar{u}_L \left(\frac{\sqrt{2}}{v\tan\beta} V m_d^D - \frac{1}{\sin\beta} V \tilde{\xi}^d \right) d_R \right] H^+ \\
& + h.c., \tag{5.1}
\end{aligned}$$

where flavor indices are omitted and the non-diagonal coupling matrices are defined as

$$\tilde{\xi}^u = U_L^\dagger \frac{1}{\sqrt{2}} \begin{pmatrix} 0 & 0 & 0 \\ 0 & 0 & 0 \\ \tilde{y}_{31}^u & \tilde{y}_{32}^u & 0 \end{pmatrix} U_R, \quad \tilde{\xi}^d = D_L^\dagger \frac{1}{\sqrt{2}} \begin{pmatrix} 0 & 0 & \tilde{y}_{13}^d \\ 0 & 0 & \tilde{y}_{23}^d \\ 0 & 0 & 0 \end{pmatrix} D_R. \quad (5.2)$$

Under the approximation $V \simeq D_L$ and $D_R \simeq \mathbf{1}$, we obtain

$$\tilde{\xi}^d \simeq V^\dagger \xi^d \simeq \frac{\sqrt{2}}{\cos \beta} \frac{m_b}{v} \begin{pmatrix} 0 & 0 & -V_{td}^* V_{tb} \\ 0 & 0 & -V_{ts}^* V_{tb} \\ 0 & 0 & 1 - |V_{tb}|^2 \end{pmatrix}. \quad (5.3)$$

References

- [1] S. Descotes-Genon, J. Matias, M. Ramon and J. Virto, *JHEP* **1301**, 048 (2013) [arXiv:1207.2753 [hep-ph]].
- [2] R. Aaij *et al.* [LHCb Collaboration], *JHEP* **1602**, 104 (2016) [arXiv:1512.04442 [hep-ex]].
- [3] R. Aaij *et al.* [LHCb Collaboration], *Phys. Rev. Lett.* **111**, 191801 (2013) [arXiv:1308.1707 [hep-ex]].
- [4] A. Abdesselam *et al.* [Belle Collaboration], arXiv:1604.04042 [hep-ex].
- [5] S. Wehle *et al.* [Belle Collaboration], arXiv:1612.05014 [hep-ex].
- [6] G. Hiller and F. Kruger, *Phys. Rev. D* **69**, 074020 (2004) [hep-ph/0310219].
- [7] C. Bobeth, G. Hiller and G. Piranishvili, *JHEP* **0712**, 040 (2007) [arXiv:0709.4174 [hep-ph]].
- [8] R. Aaij *et al.* [LHCb Collaboration], *Phys. Rev. Lett.* **113**, 151601 (2014) [arXiv:1406.6482 [hep-ex]].
- [9] R. Aaij *et al.* [LHCb Collaboration], arXiv:1705.05802 [hep-ex].
- [10] W. Altmannshofer, C. Niehoff, P. Stangl and D. M. Straub, *Eur. Phys. J. C* **77**, no. 6, 377 (2017) [arXiv:1703.09189 [hep-ph]].
- [11] B. Capdevila, A. Crivellin, S. Descotes-Genon, J. Matias and J. Virto, *JHEP* **1801**, 093 (2018) [arXiv:1704.05340 [hep-ph]].
- [12] M. Ciuchini, A. M. Coutinho, M. Fedele, E. Franco, A. Paul, L. Silvestrini and M. Valli, *Eur. Phys. J. C* **77**, no. 10, 688 (2017) [arXiv:1704.05447 [hep-ph]].
- [13] A. K. Alok, B. Bhattacharya, A. Datta, D. Kumar, J. Kumar and D. London, *Phys. Rev. D* **96**, no. 9, 095009 (2017) [arXiv:1704.07397 [hep-ph]].
- [14] A. Crivellin, G. D'Ambrosio and J. Heeck, *Phys. Rev. D* **91**, no. 7, 075006 (2015) [arXiv:1503.03477 [hep-ph]].
- [15] D. Aristizabal Sierra, F. Staub and A. Vicente, *Phys. Rev. D* **92**, no. 1, 015001 (2015) [arXiv:1503.06077 [hep-ph]].
- [16] A. Greljo, G. Isidori and D. Marzocca, *JHEP* **1507**, 142 (2015) [arXiv:1506.01705 [hep-ph]].
- [17] S. M. Boucenna, A. Celis, J. Fuentes-Martin, A. Vicente and J. Virto, *Phys. Lett. B* **760**, 214 (2016) [arXiv:1604.03088 [hep-ph]].

- [18] S. M. Boucenna, A. Celis, J. Fuentes-Martin, A. Vicente and J. Virto, JHEP **1612**, 059 (2016) [arXiv:1608.01349 [hep-ph]].
- [19] W. Altmannshofer, S. Gori, S. Profumo and F. S. Queiroz, JHEP **1612**, 106 (2016) [arXiv:1609.04026 [hep-ph]].
- [20] P. Ko, T. Nomura and H. Okada, Phys. Lett. B **772**, 547 (2017) [arXiv:1701.05788 [hep-ph]].
- [21] P. Ko, Y. Omura, Y. Shigekami and C. Yu, Phys. Rev. D **95**, no. 11, 115040 (2017) [arXiv:1702.08666 [hep-ph]].
- [22] P. Ko, T. Nomura and H. Okada, Phys. Rev. D **95**, no. 11, 111701 (2017) [arXiv:1702.02699 [hep-ph]].
- [23] E. Megias, M. Quiros and L. Salas, JHEP **1707**, 102 (2017) [arXiv:1703.06019 [hep-ph]].
- [24] S. Di Chiara, A. Fowlie, S. Fraser, C. Marzo, L. Marzola, M. Raidal and C. Spethmann, Nucl. Phys. B **923**, 245 (2017) [arXiv:1704.06200 [hep-ph]].
- [25] R. Alonso, P. Cox, C. Han and T. T. Yanagida, Phys. Rev. D **96**, no. 7, 071701 (2017) [arXiv:1704.08158 [hep-ph]].
- [26] Y. Tang and Y. L. Wu, Chin. Phys. C **42**, no. 3, 033104 (2018) [arXiv:1705.05643 [hep-ph]].
- [27] R. Alonso, P. Cox, C. Han and T. T. Yanagida, Phys. Lett. B **774**, 643 (2017) [arXiv:1705.03858 [hep-ph]].
- [28] C. W. Chiang, X. G. He, J. Tandean and X. B. Yuan, Phys. Rev. D **96**, no. 11, 115022 (2017) [arXiv:1706.02696 [hep-ph]].
- [29] C. H. Chen and T. Nomura, Phys. Lett. B **777**, 420 (2018) [arXiv:1707.03249 [hep-ph]].
- [30] S. Baek, Phys. Lett. B **781**, 376 (2018) [arXiv:1707.04573 [hep-ph]].
- [31] L. Bian, S. M. Choi, Y. J. Kang and H. M. Lee, Phys. Rev. D **96**, no. 7, 075038 (2017) [arXiv:1707.04811 [hep-ph]].
- [32] G. Faisel and J. Tandean, JHEP **1802**, 074 (2018) [arXiv:1710.11102 [hep-ph]].
- [33] S. Descotes-Genon, M. Moscati and G. Ricciardi, Phys. Rev. D **98**, no. 11, 115030 (2018) [arXiv:1711.03101 [hep-ph]].
- [34] L. Bian, H. M. Lee and C. B. Park, Eur. Phys. J. C **78**, no. 4, 306 (2018) [arXiv:1711.08930 [hep-ph]].
- [35] M. Chala and M. Spannowsky, Phys. Rev. D **98**, no. 3, 035010 (2018) [arXiv:1803.02364 [hep-ph]].
- [36] A. Falkowski, S. F. King, E. Perdomo and M. Pierre, JHEP **1808**, 061 (2018) [arXiv:1803.04430 [hep-ph]].
- [37] L. Darne, K. Kowalska, L. Roszkowski and E. M. Sessolo, JHEP **1810**, 052 (2018) [arXiv:1806.06036 [hep-ph]].
- [38] S. Baek and C. Yu, JHEP **1811**, 054 (2018) [arXiv:1806.05967 [hep-ph]].
- [39] D. Guadagnoli, M. Reboud and O. Sumensari, JHEP **1811**, 163 (2018) [arXiv:1807.03285 [hep-ph]].
- [40] G. H. Duan, X. Fan, M. Frank, C. Han and J. M. Yang, Phys. Lett. B **789**, 54 (2019) [arXiv:1808.04116 [hep-ph]].

- [41] R. H. Benavides, L. Munoz, W. A. Ponce, O. Rodriguez and E. Rojas, arXiv:1812.05077 [hep-ph].
- [42] C. Q. Geng and H. Okada, arXiv:1812.07918 [hep-ph].
- [43] P. T. P. Hutaeruk, T. Nomura, H. Okada and Y. Orikasa, arXiv:1901.03932 [hep-ph].
- [44] S. Baek, arXiv:1901.04761 [hep-ph].
- [45] M. Tanabashi *et al.* [Particle Data Group], Phys. Rev. D **98**, no. 3, 030001 (2018).
- [46] P. Langacker, Rev. Mod. Phys. **81**, 1199 (2009) [arXiv:0801.1345 [hep-ph]].
- [47] L. M. Krauss and F. Wilczek, Phys. Rev. Lett. **62**, 1221 (1989).
- [48] M. Aaboud *et al.* [ATLAS Collaboration], JHEP **1811**, 085 (2018) [arXiv:1808.03599 [hep-ex]].
- [49] A. M. Baldini *et al.* [MEG Collaboration], Eur. Phys. J. C **76**, no. 8, 434 (2016) [arXiv:1605.05081 [hep-ex]].
- [50] A. M. Baldini *et al.* [MEG II Collaboration], Eur. Phys. J. C **78**, no. 5, 380 (2018) [arXiv:1801.04688 [physics.ins-det]].
- [51] Y. Kuno and Y. Okada, Rev. Mod. Phys. **73**, 151 (2001) [hep-ph/9909265].
- [52] R. Kitano, M. Koike and Y. Okada, Phys. Rev. D **66**, 096002 (2002) Erratum: [Phys. Rev. D **76**, 059902 (2007)] [hep-ph/0203110].
- [53] S. Davidson, Y. Kuno and M. Yamanaka, arXiv:1810.01884 [hep-ph].
- [54] T. Suzuki, D. F. Measday and J. P. Roalsvig, Phys. Rev. C **35**, 2212 (1987).
- [55] W. H. Bertl *et al.* [SINDRUM II Collaboration], Eur. Phys. J. C **47**, 337 (2006).
- [56] Y. Kuno [COMET Collaboration], PTEP **2013**, 022C01 (2013). doi:10.1093/ptep/pts089
- [57] R. M. Carey *et al.* [Mu2e Collaboration], FERMILAB-PROPOSAL-0973
- [58] I. Bediaga *et al.* [LHCb Collaboration], CERN-LHCC-2012-007, LHCb-TDR-12.
- [59] E. Kou *et al.* [Belle II Collaboration], arXiv:1808.10567 [hep-ex].
- [60] W. Altmannshofer, S. Gori, M. Pospelov and I. Yavin, Phys. Rev. Lett. **113**, 091801 (2014) [arXiv:1406.2332 [hep-ph]].
- [61] G. W. Bennett *et al.* [Muon G-2 Collaboration], Phys. Rev. D **73**, 072003 (2006) [hep-ex/0602035].
- [62] P. Arnan, L. Hofer, F. Mescia and A. Crivellin, JHEP **1704**, 043 (2017) [arXiv:1608.07832 [hep-ph]].
- [63] A. Bazavov *et al.* [Fermilab Lattice and MILC Collaborations], Phys. Rev. D **93**, no. 11, 113016 (2016) [arXiv:1602.03560 [hep-lat]].
- [64] P. Ko, Y. Omura and C. Yu, Phys. Rev. D **85**, 115010 (2012) [arXiv:1108.0350 [hep-ph]].
- [65] P. Ko, Y. Omura and C. Yu, JHEP **1201**, 147 (2012) [arXiv:1108.4005 [hep-ph]].
- [66] P. Ko, Y. Omura and C. Yu, Eur. Phys. J. C **73**, no. 1, 2269 (2013) [arXiv:1205.0407 [hep-ph]].
- [67] P. Ko, Y. Omura and C. Yu, JHEP **1303**, 151 (2013) [arXiv:1212.4607 [hep-ph]].

- [68] B. Capdevila, A. Crivellin, S. Descotes-Genon, L. Hofer and J. Matias, Phys. Rev. Lett. **120**, no. 18, 181802 (2018) [arXiv:1712.01919 [hep-ph]].
- [69] J. P. Lees *et al.* [BaBar Collaboration], Phys. Rev. Lett. **118**, no. 3, 031802 (2017) [arXiv:1605.09637 [hep-ex]].
- [70] A. Belyaev, N. D. Christensen and A. Pukhov, Comput. Phys. Commun. **184**, 1729 (2013) [arXiv:1207.6082 [hep-ph]].
- [71] P. M. Nadolsky, H. L. Lai, Q. H. Cao, J. Huston, J. Pumplin, D. Stump, W. K. Tung and C.-P. Yuan, Phys. Rev. D **78**, 013004 (2008) [arXiv:0802.0007 [hep-ph]].
- [72] M. Aaboud *et al.* [ATLAS Collaboration], JHEP **1710**, 182 (2017) [arXiv:1707.02424 [hep-ex]].
- [73] V. Khachatryan *et al.* [CMS Collaboration], JHEP **1702** (2017) 048 [arXiv:1611.06594 [hep-ex]].
- [74] M. Aaboud *et al.* [ATLAS Collaboration], JHEP **1801**, 126 (2018) [arXiv:1711.03301 [hep-ex]].
- [75] G. Belanger, F. Boudjema, A. Pukhov and A. Semenov, Comput. Phys. Commun. **192**, 322 (2015) [arXiv:1407.6129 [hep-ph]].
- [76] N. Aghanim *et al.* [Planck Collaboration], arXiv:1807.06209 [astro-ph.CO].
- [77] A. Albert *et al.* [Fermi-LAT and DES Collaborations], Astrophys. J. **834**, no. 2, 110 (2017) [arXiv:1611.03184 [astro-ph.HE]].
- [78] S. Hoof, A. Geringer-Sameth and R. Trotta, arXiv:1812.06986 [astro-ph.CO].